

## Flexible In-Ga-Zn-O thin-film transistors with sub-300-nm channel lengths defined by two-photon direct laser writing

Article (Accepted Version)

Petti, Luisa, Greco, Emanuel, Cantarella, Giuseppe, Munzenrieder, Niko, Vogt, Christian and Troster, Gerhard (2018) Flexible In-Ga-Zn-O thin-film transistors with sub-300-nm channel lengths defined by two-photon direct laser writing. *IEEE Transactions on Electron Devices*, 35 (9). pp. 3796-3802. ISSN 0018-9383

This version is available from Sussex Research Online: <http://sro.sussex.ac.uk/id/eprint/77473/>

This document is made available in accordance with publisher policies and may differ from the published version or from the version of record. If you wish to cite this item you are advised to consult the publisher's version. Please see the URL above for details on accessing the published version.

### **Copyright and reuse:**

Sussex Research Online is a digital repository of the research output of the University.

Copyright and all moral rights to the version of the paper presented here belong to the individual author(s) and/or other copyright owners. To the extent reasonable and practicable, the material made available in SRO has been checked for eligibility before being made available.

Copies of full text items generally can be reproduced, displayed or performed and given to third parties in any format or medium for personal research or study, educational, or not-for-profit purposes without prior permission or charge, provided that the authors, title and full bibliographic details are credited, a hyperlink and/or URL is given for the original metadata page and the content is not changed in any way.

# Flexible In-Ga-Zn-O Thin-Film Transistors with sub-300 nm Channel Lengths Defined by Two-Photon Direct Laser Writing

L. Petti, E. Greco, G. Cantarella, N. Münzenrieder, *Member, IEEE*, C. Vogt, *Student Member, IEEE*  
and G. Tröster, *Senior Member, IEEE*

**Abstract**—In this work, the low-temperature ( $\leq 150$  °C) fabrication and characterization of flexible Indium-Gallium-Zinc-Oxide (IGZO) top-gate thin-film transistors (TFTs) with channel lengths down to 280 nm is presented. Such extremely short channel lengths in flexible IGZO TFTs were realized with a novel manufacturing process combining two-photon direct laser writing (DLW) photolithography with Ti/Au/Ti source/drain e-beam evaporation and lift-off. The resulting flexible IGZO TFTs exhibit a saturation field-effect mobility of  $1.1 \text{ cm}^2\text{V}^{-1}\text{s}^{-1}$  and a threshold voltage of 3 V. Thanks to the short channel lengths (280 nm) and the small gate to source/drain overlap (5.2  $\mu\text{m}$ ), the TFTs yield a transit frequency of 80 MHz (at 8.5 V gate-source voltage) extracted from the measured S-parameters. Furthermore, the devices are fully functional when wrapped around a cylindrical rod with 6 mm radius, corresponding to 0.4 % tensile strain in the TFT channel. These results demonstrate a new methodology to realize entirely flexible nano-structures, and prove its suitability for the fabrication of short-channel transistors on polymer substrates for future wearable communication electronics.

**Index Terms**— Flexible electronics, indium–gallium–zinc oxide (IGZO), thin-film transistor, transit frequency, mechanical strain.

## I. INTRODUCTION

The advances flexible and stretchable devices have made over the last decades are enabling a wide range of novel applications, such as wearable and textile integrated devices [1, 2], seamlessly embedded patch-like systems [3], artificial and soft robotic skins [4], as well as imperceptible and transient medical implants [5]. This fuels the quest for thin-film

transistors (TFTs) combining excellent electrical performance with extreme mechanical bendability, as well as low temperature processability. Among state-of-the-art semiconducting materials, Indium-Gallium-Zinc-Oxide (IGZO) is currently one of the most promising option, owing to the carrier mobility typically above  $10 \text{ cm}^2\text{V}^{-1}\text{s}^{-1}$  even when processed at room-temperature [6], as well as the mechanical bendability down to radii as small as 20  $\mu\text{m}$  [7]. While electrical DC performance and mechanical properties of flexible IGZO TFTs have been extensively explored [8], the AC characteristic of flexible IGZO devices has been significantly less investigated. This is mainly due to the challenges involved in the realization of short-channel and high-frequency TFTs on flexible substrates [8]. To date, flexible IGZO TFTs with channel lengths below 1  $\mu\text{m}$  have been realized either using self-alignment [9] or vertical [10] and quasi-vertical [11] device structures. In particular, self-alignment of the source/drain contacts to the gate allowed fabricating bottom-gate (BG) IGZO TFTs with channel lengths of 500 nm yielding a field-effect mobility  $\mu_{\text{FE}}$  of  $7.5 \text{ cm}^2\text{V}^{-1}\text{s}^{-1}$  and a transit frequency  $f_{\text{T}}$  of 135 MHz. Shorter channels lengths of 300 nm have only been achieved using a quasi-vertical TFT (QVTFT) architecture [11]. However, process-induced source/drain contact contamination in the IGZO QVTFT structure resulted in large contact resistance of 45  $\Omega\text{cm}$ , low field-effect mobility of  $0.2 \text{ cm}^2\text{V}^{-1}\text{s}^{-1}$ , and thereby low transit frequency of 1.5 MHz. The reduced  $f_{\text{T}}$  illustrates how for short-channel TFTs, the channel resistance becomes comparable and eventually smaller than the contact resistance, resulting in a consequent  $\mu_{\text{FE}}$  drop [12]. In general, this limits the AC performance of both planar and vertical IGZO TFTs. Nevertheless, the effective mobility degradation encountered in flexible planar IGZO TFTs is not as pronounced as in vertical devices [8]. Additionally, in vertical TFTs the optimization of the parasitic overlap between gate and source/drain contacts (which is another key parameter impacting the AC performance [12]) is further complicated by the device structure. This is why there is a strong need for alternative fabrication processes enabling short channel lengths ( $\ll 500$  nm) in flexible planar IGZO TFTs. While electron beam (e-beam) lithography is especially suitable for the miniaturization of electronic devices on traditional semiconductor wafers, to

Manuscript submitted on April, 20, 2018. This work was supported by the SNF/DFG DACH FFLexCom project: Wireless Indium-Gallium Transmitters and Devices on Mechanically Flexible Thin-Film Substrates (WISDOM, SNF grant number 160347).

L. Petti, E. Greco, G. Cantarella, N. Münzenrieder, C. Vogt, and G. Tröster are with the Institute for Electronics at the Swiss Federal Institute of Technology Zürich, Zürich, 8092, Switzerland (email: luisa.petti@ife.ee.ethz.ch; ema89gre@gmail.com; giuseppe.cantarella@ife.ee.ethz.ch; muenzenrieder@ife.ee.ethz.ch; christian.vogt@ife.ee.ethz.ch; troester@ife.ee.ethz.ch)

N. Münzenrieder is with the Sensor Technology Research Center, School of Engineering and Informatics at the University of Sussex, Richmond 3A7, Falmer, Brighton, BN1 9QT, United Kingdom (email: N.S.Munzenrieder@sussex.ac.uk)

the best our knowledge its use on flexible plastic substrates has never been proven. In fact, the non-perfectly flat nature of plastic foils requires precise adjustments of the focal point as close as possible to the exposure area. Such adjustments are not possible in e-beam lithographic systems, due to the resulting un-intended illumination of the photo-resist. Furthermore, the typically non-conductive properties of flexible plastic substrates lead to charging effects which further challenge the process of focalization. Deposition of thin conductive layers on the insulating substrates is possible, at a cost of reduced overall thickness and increased process complexity. To this regard, two-photon direct laser writing (DLW) [13] has been proposed as an attractive tool for the realization of two-dimensional (2D) and three-dimensional (3D) micro- and nano-structures for a wide range of applications, from optical interconnects [14], photonics [15], micro-fluidics [16], to cell scaffolds and bio-mimetics [17]. Recently, also conductive 3D Au-based micro-structures have been fabricated by two-photon DLW [18]. However, to the best of our knowledge, two-photon DLW has not yet been utilized for the 2D miniaturization of TFT channels on flexible substrates. Main advantage of two-photon DLW as compared to e-beam lithography for 2D nano-structuring on free-standing flexible plastic substrates is the possibility to precisely adjust the focal point in the exposure area without un-intentional illumination of the photoresist.

In this paper, we report the use of two-photon DLW for the fabrication of planar IGZO TFTs with channel lengths down to 280 nm on a flexible polyimide substrate. The presented TFTs exhibit a contact resistance  $r_C$  of 22  $\Omega\text{cm}$  and a saturation field effect mobility  $\mu_{\text{SAT}}$  of  $1.1 \text{ cm}^2\text{V}^{-1}\text{s}^{-1}$ . The short IGZO channel length in combination with the small gate to source/drain overlap length ( $L_{\text{OV}} = 5.2 \mu\text{m}$ ) results in a transit frequency of 80 MHz (at 8.5 V gate-source voltage). Furthermore, flexible IGZO TFTs with channels defined by two-photon DLW are fully operational when bent to 6 mm radii, corresponding to 0.4% tensile strain applied parallel to the device channel. Part of the work presented here is based on preliminary results reported in the doctoral thesis of the main author [19].

## II. FABRICATION PROCESS

Flexible IGZO TFTs with DLW-defined channels were fabricated on 50  $\mu\text{m}$ -thick Kapton E polyimide (PI) foil (surface area:  $2.5 \times 2.5 \text{ cm}^2$ ). The devices are based on a top-gate bottom-contact (TG-BC) TFT structure, as shown in Fig. 1. The TFT manufacturing process uses a maximum process temperature of 150  $^\circ\text{C}$  and is schematically illustrated in Fig. 2.

The fabrication process starts with the plasma enhanced chemical vapor deposition of 50 nm  $\text{SiN}_x$  on the PI foil, acting as adhesion layer. Next, to allow a reliable structuring of the TFT channels in the photoresist by DLW photolithography, the flexible PI substrate was attached to a glass carrier using double-sided tape (Fig. 2 (a)) and subsequently coated with a drop-casted IP-Dip photoresist. IP-Dip is a negative photoresist (from Nanoscribe GmbH) that behaves very similar

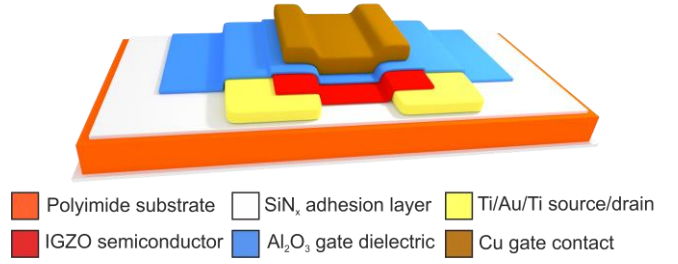


Fig. 1. Schematic cross-section of the top-gate bottom-contact (TG-BC) In-Ga-Zn-O (IGZO) thin-film-transistors (TFTs) with channels defined via two-photon direct laser writing (DLW) on flexible polyimide substrates.

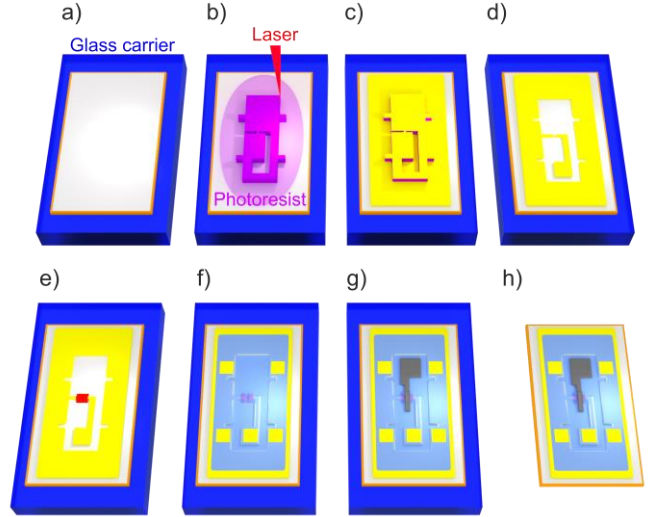


Fig. 2. Manufacturing process flow of flexible TG-BC IGZO TFTs with channels defined via two-photon DLW. (a)  $\text{SiN}_x$  adhesion layer deposition by plasma enhanced chemical vapor deposition and subsequent mounting of flexible polyimide (PI) substrate on glass carrier using double-sided tape. (b) Drop-casting, DLW illumination and development of photoresist. (c) E-beam evaporation of Ti/Au/Ti source and drain contacts. (d) Channel and source/drain contact structuring by lift-off. (e) RF magnetron sputtering and wet etching of IGZO semiconductor. (f) Atomic layer deposition and wet etching of  $\text{Al}_2\text{O}_3$  gate dielectric. (g) E-beam evaporation and wet etching of Cu TG electrode. (h) PI substrate demounting from glass carrier resulting in free-standing flexible TFTs with channel lengths as small as 280 nm.

to SU-8 and other acrylate-based negative resists [20]. The main feature of using IP-Dip in combination with two-photon DLW photolithography [21] is that minimum line widths down to 150 nm can be structured in the photoresist [20]. For the DLW photolithography, the photonic professional system from NanoScribe GmbH was utilized. This is a system based on two-photon polymerization with ultra-short laser pulses [22], where 2D and 3D micro- and nano-structures are written following laser paths connected from the beginning to the end of the writing process [20]. This is why prior to the DLW photolithographic process, an optimized computer-aided design (CAD) of the laser paths required to structure the desired TFT channels (Fig. 2(b)) was generated. The channel structures displayed in Fig. 2(b) were patterned into the drop-casted IP-Dip photoresist by directly exposing the photoresist – using the so-called dip-in-lithography (DILL) configuration [21] – utilizing an optimized laser power of 4.6  $\mu\text{W}$ . In

particular, the exposure of the entire source and drain pattern shown in Fig. 2(b) was split in three main structures, to allow a precise focal point adjustment at the beginning of each structure, as well as an exposure height reduction in the thin and long channel area (to increase mechanical stability). The subsequent IP-Dip development resulted in channel stripes 280 nm wide and 17  $\mu\text{m}$  long patterned in the negative photoresist (Fig. 2(b)).

Following the two-photon DLW process, a layer of Ti/Au/Ti (10 nm/60 nm/10 nm) was e-beam evaporated (Fig. 2(c)). The subsequent lift-off process removed the IP-Dip photoresist and defined the channel areas, as well as the source and drain contacts (Fig. 2(d)). Then, a 15 nm-thick IGZO film was RF magnetron sputtered (at room temperature) from a ceramic InGaZnO<sub>4</sub> target and structured into small semiconductor islands (19 x 20  $\mu\text{m}^2$ ) by wet etching (Fig. 2(e)). Afterwards, an 80 nm-thick Al<sub>2</sub>O<sub>3</sub> film (dielectric constant: 9.5) was grown by atomic layer deposition (ALD) at 150 °C and wet etched to open source/drain contact holes (Fig. 2(f)). In this case, the 80 nm-thick Al<sub>2</sub>O<sub>3</sub> film represents a trade-off between high field effect mobility and low-voltage TFT operation [8]. Due to the TG-BC device structure, the Al<sub>2</sub>O<sub>3</sub> film acts as both gate dielectric and channel passivation layer. Subsequently, 100 nm of Cu were e-beam evaporated and patterned in gate contacts using wet chemistry (Fig. 2(g)). Finally, the PI foil was detached from the glass carrier leading to free-standing flexible IGZO TFTs with channel lengths as small as 280 nm.

Fig. 3(a) displays an optical micrograph of one device, which uses a ground-signal-ground (GSG) layout to allow AC characterization. SEM enlargements of the TFT channel in Fig. 3(b) and (c) show the TFT dimensions with a channel length  $L = 280$  nm, a channel width  $W = 17$   $\mu\text{m}$  and a gate to source/drain overlap length  $L_{OV} = 5.2$   $\mu\text{m}$ . A minor slanting of the profile of the inner edges of the source and drain contacts as compared to outer edges (Fig. 3(c)) is caused by the still limited mechanical stability of the 280 nm wide, 17  $\mu\text{m}$  long and 1.7  $\mu\text{m}$  thick IP-Dip channel stripes during the photoresist development and subsequent Ti/Au/Ti evaporation and lift-off. The non-perfectly defined inner edges of the source/drain contacts (Figure 3(c)) are due to the small-sized pattern, as well as due to small particles on the Polyimide/SiNx/IP-Dip surface and/or on the Polyimide/SiNx/IP-Dip/Ti/Au/Ti surface originating during the fabrication process. Furthermore, non-perfectly defined edges of the surrounding source metal (Fig. 3(a)) can be explained by the photoresist DLW exposure process divided in three sequences with different thicknesses of the IP-Dip exposed areas and different focal point adjustments.

On each  $2.5 \times 2.5$  cm<sup>2</sup> PI foil, up to 9 GSG devices with different channel lengths and widths can be realized with the presented manufacturing process (Fig. 2). A larger number of TFTs is currently limited by the DLW laser defining the entire GSG source/drain structure for each TFT. However, in the future the DLW laser could be used to structure the TFT channels only, whereas the remaining source/drain patterns could be realized using an UV photolithographic and wet

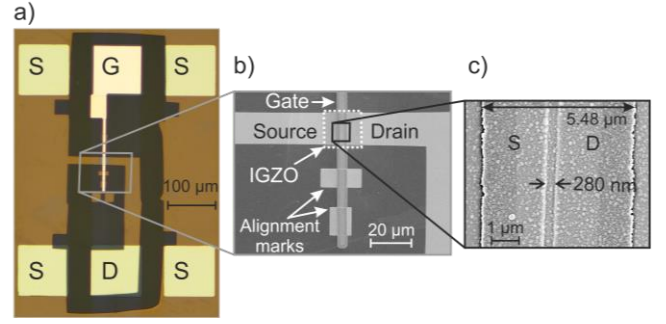


Fig. 3. (a) Optical micrograph of a complete flexible TG-BC IGZO TFT with channel defined via two-photon DLW showing the employed ground-signal-ground (GSG) layout of the contact pads. All six contact pads have a size of 100  $\mu\text{m} \times 100$   $\mu\text{m}$ . (b) SEM micrograph of the TFT channel area. (c) SEM top view of the channel used to determine the exact channel length of 280 nm. Samples were coated with 10-nm Pt to create a sufficient electrical conductivity on the insulating substrate.

TABLE I  
TFT PERFORMANCE PARAMETERS

Parameter	Value
Saturation Field Effect Mobility $\mu_{\text{SAT}}$	1.1 cm <sup>2</sup> V <sup>-1</sup> s <sup>-1</sup>
Threshold Voltage $V_{\text{TH}}$	3 V
On/Off Current Ratio $I_{\text{ON}}/I_{\text{OFF}}$ ( $V_{\text{GS}} = 2.1$ V)	10 <sup>3</sup>
Sub-threshold Swing SS	2 V/dec
Transconductance $g_m$ ( $V_{\text{GS}} = 9$ V, $V_{\text{DS}} = 5.1$ V)	250 $\mu\text{S}$
Output Conductance $g_{\text{ds}}$ ( $V_{\text{GS}} = 7$ V, $V_{\text{DS}} = 5.1$ V)	12 $\mu\text{S}$
Internal Gain $g_m/g_{\text{ds}}$ ( $V_{\text{GS}} = 7$ V, $V_{\text{DS}} = 5.1$ V)	2.9
Contact Resistance $R_c$	22 $\Omega\text{cm}$
Gate Capacitance $C_g$	487 fF
Transit Frequency $f_T$	80 MHz

etching step after the lift-off process of the short channels (Fig. 2(d)). This additional step combined with the use of Cr/Au/Cr source/drain contacts [23] would also allow realizing standard IGZO TG-BC TFTs with longer channels ( $L > 1$   $\mu\text{m}$ ) [23] on the same substrate. This would be especially relevant for high-frequency analog circuits, where only a few amplifying TFTs require short channels, whereas all other components are typically designed with much longer channels [24].

### III. CHARACTERIZATION

#### A. DC Characterization

The devices were characterized under ambient conditions using an Agilent technologies B1500A parameter analyzer. The corresponding TFT performance parameters (Table 1) were extracted using standard transistor equations [8].

Fig. 4 shows the  $I_D$ - $V_{\text{GS}}$  transfer (a) and  $I_D$ - $V_{\text{DS}}$  output (b) characteristic of a flexible IGZO TFT with channel length and width of 280 nm and 17  $\mu\text{m}$ , respectively. Based on the transfer characteristic measurements (Fig. 4(a)), the following DC performance parameters (see Table 1) were extracted: a saturation field-effect mobility  $\mu_{\text{SAT}}$  of 1.1 cm<sup>2</sup>V<sup>-1</sup>s<sup>-1</sup> (at  $V_{\text{DS}} = 5.1$  V), a threshold voltage  $V_{\text{TH}}$  of 3 V, an on/off current ratio  $I_{\text{ON}}/I_{\text{OFF}}$  of  $7 \times 10^1$  (at  $V_{\text{DS}} = 5.1$  V), a sub-threshold swing SS of 2 V/dec, and a maximum tranconductance  $g_m$  (see Figure



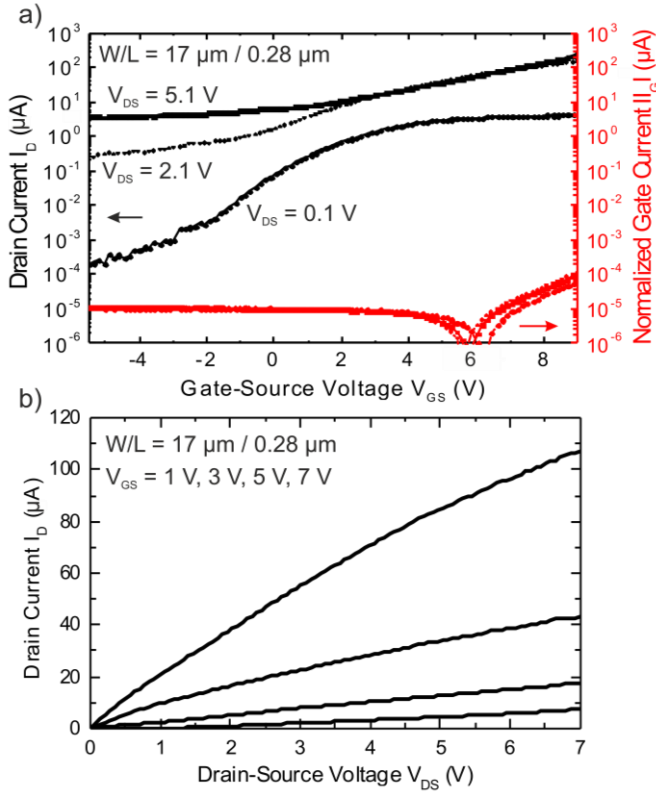


Fig. 4. Flexible IGZO TFT with channel defined via two-photon DLW (channel length  $L$  and width  $W$  of 0.28 and 17  $\mu\text{m}$ , respectively): transfer (a) and output (b) characteristic.

5(a)) of 250  $\mu\text{S}$  (at  $V_{\text{GS}} = 9 \text{ V}$  and  $V_{\text{DS}} = 5.1 \text{ V}$ ). Flexible short-channel IGZO TFTs with DLW-defined channels exhibit significantly larger  $\mu_{\text{SAT}}$  if compared to flexible IGZO QVTFTs with similarly short channel lengths [11]. This is mainly due to approximately halved contact resistance ( $r_c = 22 \Omega\text{cm}$ ) that planar TG IGZO TFTs ( $L = 280 \text{ nm}$ ) yield compared to IGZO QVTFTs ( $L = 300 \text{ nm}$ ) [11]. The extracted  $r_c$  of 22  $\Omega\text{cm}$  is only slightly higher than state-of-the-art values of 12.5  $\Omega\text{cm}$  obtained for flexible self-aligned IGZO BG TFTs ( $L = 500 \text{ nm}$ ) [9, 12]. This slight increase is mainly attributed to the more contaminated interface between IGZO and Ti/Au/Ti source/drain contacts in the TG-BC device structure. A 1.8 $\times$  larger contact resistance, combined with a 1.8 $\times$  shorter channel length explains why TG IGZO TFTs with DLW-defined channels yield a 6.8 $\times$  lower saturation mobility compared to self-aligned BG IGZO devices with 500 nm long channels.

As shown in Fig. 4(a), the off current  $I_{\text{OFF}}$  always exceeds 100 pA, and further increases with higher drain-source voltages up to  $I_{\text{OFF}} = 1 \mu\text{A}$  at  $V_{\text{DS}} = 5.1 \text{ V}$  (Fig. 4(a)). Such large off current (leading to small  $I_{\text{ON}}/I_{\text{OFF}}$ ) is mainly attributed to the poor electrostatic control in the 280 nm short channel. A reduction in the IGZO island size, as well as a better definition of the inner edges of the source/drain contacts (Figure 3(c)) is expected to improve the electrostatic control of the lateral S/D field and therefore the on/off ratio of our short-channel TFTs.

Sufficient saturation performance for larger  $V_{\text{DS}}$  (Fig. 4(b)) is demonstrated also by the similar on current performance of the transfer curves (Fig. 4(a)) at  $V_{\text{GS}} = 2.1 \text{ V}$  and 5.1 V.

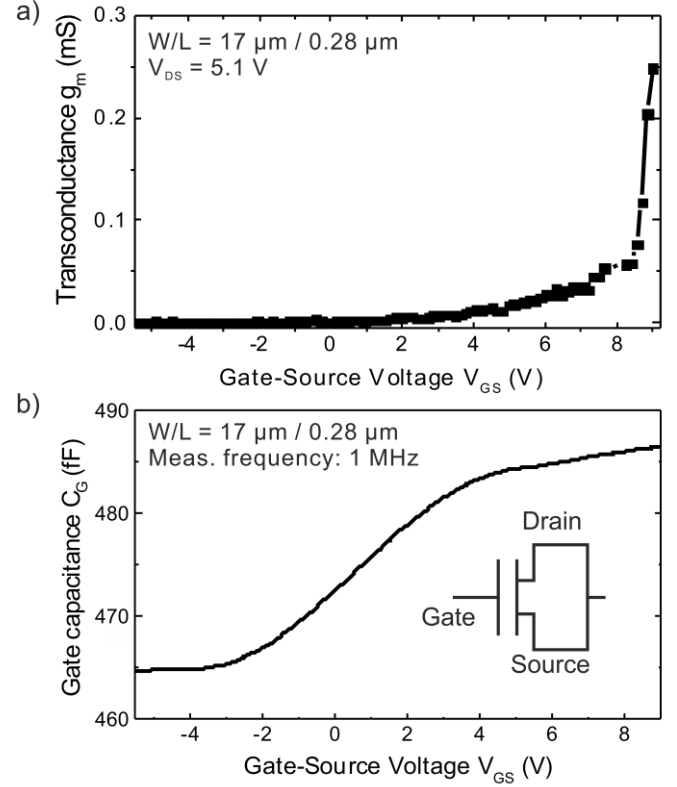


Fig. 5. Flexible IGZO TFT with channel defined via two-photon DLW (channel  $L = 0.28 \mu\text{m}$  and  $W = 17 \mu\text{m}$ ): (a) transconductance and (b) gate capacitance (measured at 1 MHz). The inset in b) shows the configuration used to measure the gate capacitance.

From the output characteristic data (Fig. 4(b)), an output conductance  $g_{\text{ds}} = 12 \mu\text{S}$  (at  $V_{\text{GS}} = 7 \text{ V}$  and  $V_{\text{DS}} = 5.1 \text{ V}$ ) was extrapolated. In combination with the correspondingly measured  $g_{\text{m}}$  value (at  $V_{\text{GS}} = 7 \text{ V}$  and  $V_{\text{DS}} = 5.1 \text{ V}$ , see Fig. 5(a)), we derived an internal gain  $g_{\text{m}}/g_{\text{ds}}$  of 2.9, which is well above the minimum gain typically required for analog circuits [12]. This proves that our short-channel IGZO TFTs are suitable for analog flexible electronic applications.

From C-V measurements (Fig. 5(b)), a gate-to source/drain overlap capacitance of 465 fF (measured at negative bias voltages  $V_{\text{GS}} = -5 \text{ V}$ ), and a total gate capacitance of 487 fF (measured in the on regime, at  $V_{\text{GS}} = 9 \text{ V}$ ) were extracted. Such low gate capacitance  $C_{\text{G}}$  values have been obtained thanks to the 80 nm-thick  $\text{Al}_2\text{O}_3$  dielectric, combined with the short channel length of 280 nm and the small total overlap between gate and source/drain  $L_{\text{OV}}$  of 5.2  $\mu\text{m}$ .

The transconductance  $g_{\text{m}}$  of 250  $\mu\text{S}$  ( $V_{\text{GS}} = 9 \text{ V}$  and  $V_{\text{DS}} = 5.1 \text{ V}$ ) and the total gate capacitance  $C_{\text{G}} = 487 \text{ fF}$  ( $V_{\text{GS}} = 9 \text{ V}$ ) enable the theoretical calculation of the TFT transit frequency  $f_{\text{T}}$  [8] (at 9 V gate-source voltage) of 81 MHz.

### B. AC Characterization

Scattering parameters (S-parameters) of the flexible IGZO TFTs with DLW-defined channels were measured using a two-port HP 8753E network analyzer. For the measurements, port one and port two of the network analyzer were respectively connected to the gate and the drain contact of the TFTs, whereas the source was grounded. Before all measurements, the system was calibrated by a full two-port calibration. An AC

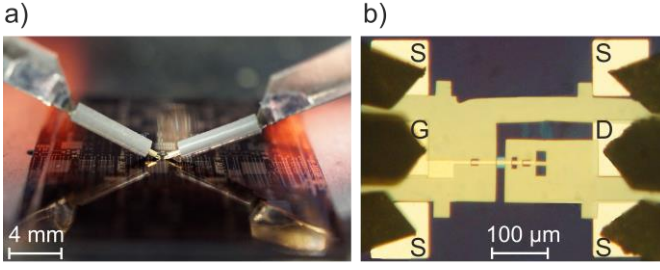


Fig. 6. (a) Photograph of a polyimide substrate with IGZO TFTs with channels defined via two-photon DLW, prepared for AC characterization with a two-port network analyzer. A single TFT contacted by 2 GSG probe tips is shown in the optical micrograph in (b).

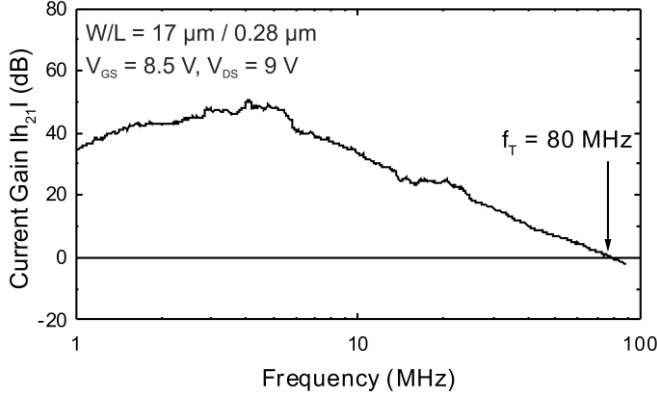


Fig. 7. Absolute value of current gain  $h_{21}$  extracted from Scattering parameters (S-parameter) measurements [25] of a flexible IGZO TFT with channel defined via two-photon DLW (channel  $L = 0.28 \mu\text{m}$  and  $W = 17 \mu\text{m}$ ). Current gain values have been averaged to reduce measurement noise. The extrapolated transit frequency  $f_T$  is 80 MHz (at  $V_{GS} = 8.5 \text{ V}$ ).

peak-to-peak voltage amplitude of 100 mV was used. Fig. 6(a) shows the flexible IGZO TFTs prepared for AC characterization using the two-port network analyzer. A micrograph of a single short-channel IGZO TFT contacted by 2 GSG probe tips is given in Fig. 6(b). Fig. 7 displays the current gain  $h_{21}$  plot, which was calculated using the measured S-parameters [25]. From the  $h_{21}$  plot, we derived a transit frequency  $f_T$  of 80 MHz which agrees with the value of 81 MHz estimated from  $g_m$  and  $C_G$  data. Compared to IGZO QVTFTs with similarly short channel lengths ( $L = 300 \text{ nm}$ ) [11], flexible IGZO TFTs with DLW-defined channels yield a  $53\times$  higher  $f_T$ . Even though the obtained frequency is lower than the  $f_T = 135 \text{ MHz}$  reported for flexible self-aligned IGZO TFTs ( $L = 500 \text{ nm}$ ) [9], the value is extremely high given the comparably low mobility and the low gate voltage. Additionally, future optimization of the source/drain contacts, combined with shorter channel and overlap lengths promises to enable higher  $\mu_{SAT}$  and  $f_T$ .

Already based on these results, two-photon DLW photolithography offers a viable route for the realization of flexible short-channel electronic devices.

#### IV. MECHANICAL STRAIN

To investigate and demonstrate the flexibility of IGZO TFTs with channels defined by two-photon DLW, mechanical bendability tests were performed. The free-standing TFTs

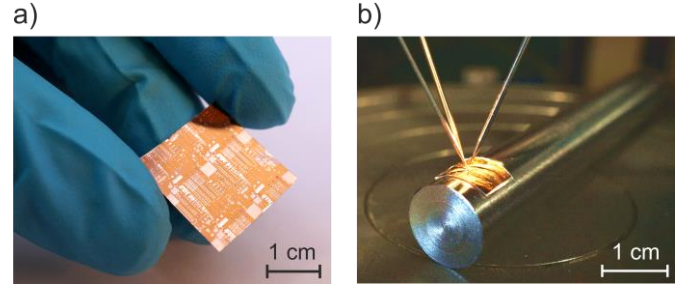


Fig. 8. Photographs of flexible polyimide substrate with IGZO TFTs with channels defined via two-photon DLW: (a) free-standing substrate cut for mechanical bendability tests and (b) substrate measured while bent to a tensile radius of 6 mm parallel to the TFT channel.

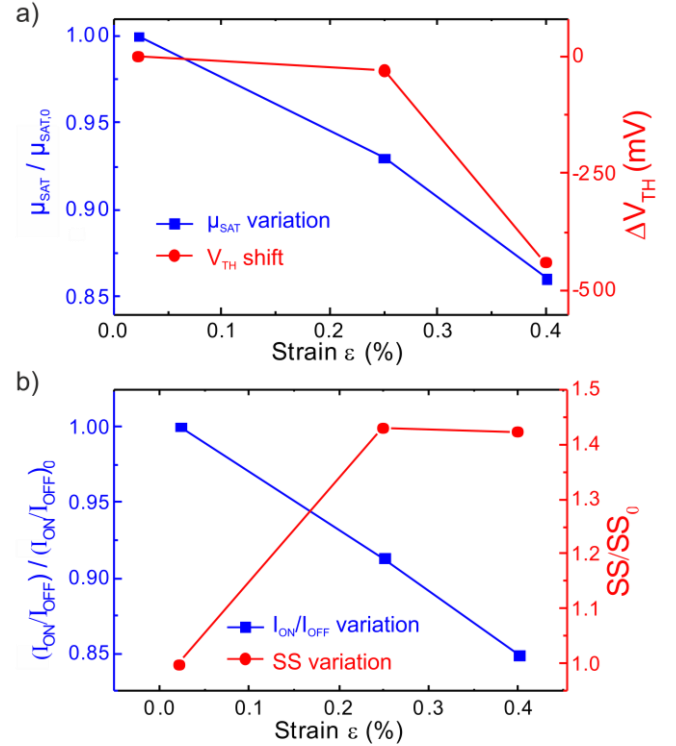


Fig. 9. Flexible IGZO TFTs with channel defined via two-photon DLW: (a) normalized saturation field-effect mobility and threshold voltage shift and (b) normalized on/off current ratio and subthreshold swing for different tensile strains (up to 0.4 %) applied parallel to the TFT channel.

(Figure 8(a)) were attached to double-sided tape and wound around cylindrical rods (Fig. 8(b)) in a way that tensile strain was applied parallel to the channel [8]. The radius of the smallest employed rod was 6 mm (Fig. 8(b)). As shown in Fig. 9, flexible IGZO TFTs with 280 nm channel lengths are fully operational while bent to tensile radii of 10 and 6 mm, corresponding to mechanical strains  $\epsilon$  of  $\approx 0.25 \%$  and  $0.4 \%$  in the TFT channel [27]. In particular, bending to  $0.4 \%$  strain yields a 14 % reduction of the effective mobility, a negative threshold voltage shift of 440 mV, a 15 % reduced on/off ratio, and a  $1.4\times$  larger sub-threshold swing. These changes can be explained by the under tensile increased resistance of the metallic contacts, which becomes dominant for short-channel lengths [8]. Bending to smaller radii leads to the formation of cracks in the extended Ti/Au/Ti metallic surface, which causes

permanent parameter shifts at 5 mm bending radii and device failure at radii < 5 mm. The introduction of an additional UV photolithographic and wet etching step after the lift-off process of the channel structures would be beneficial not only from a process perspective, but also for mechanical bendability as it would reduce the extended metallic surface and thereby increase the strain resistance of the final devices.

## V. CONCLUSION

In this work, flexible IGZO TFTs with channel lengths as small as 280 nm have been demonstrated. The, to the best of our knowledge, shortest channel length ever reported for flexible IGZO TFTs were realized using two-photon DLW photolithography. In particular, the sub-300 nm channel patterns were first defined in a specifically designed negative photoresist and subsequently transferred to the TFT source/drain contacts by lift-off of an e-beam evaporated Ti/Au/Ti film. The short channel combined with IGZO semiconductor and 80 nm Al<sub>2</sub>O<sub>3</sub> gate dielectric, resulted in TFTs with a saturation field-effect mobility of 1.1 cm<sup>2</sup>V<sup>-1</sup>s<sup>-1</sup>, a threshold voltage of 3 V, and a sub-threshold swing of 2V/dec. The 280 nm long channel together with a 5.2 μm gate to source/drain overlap enabled a transit frequency of 80 MHz, extracted from two port S-parameter measurements. In addition, the performance of the flexible short-channel TFTs was also maintained while the devices were bent down to 6 mm tensile radii, corresponding to 0.4% strain parallel to the TFT channels. The presented results confirm the suitability of IGZO TFTs [8] for high-frequency flexible electronic applications. At the same, future optimization of the manufacturing process is expected to enable even shorter channel and overlap lengths and therefore higher transit frequencies, highlighting the advantages of the newly proposed fabrication process in the field of wearable communication electronics.

## ACKNOWLEDGMENT

The authors would like to express their gratitude to Dr. David Borer for the help in the Nanoscribe DLW photolithographic process.

## REFERENCES

- [1] A. Nathan, A. Ahnood, M. T. Cole, S. Lee, Y. Suzuki, P. Hiralal, F. Bonaccorso, T. Hasan, L. Garcia-Gancedo, A. Dyadyusha, S. Haque, P. Andrew, S. Hofmann, J. Moultrie, D. Chu, A. J. Flewitt, A. C. Ferrari, M. J. Kelly, J. Robertson, G. A. J. Amaratunga, and W. I. Milne, "Flexible electronics: The next ubiquitous platform," *Proceedings of the IEEE*, vol. 100, no. 13, pp. 1486–1517, May 2012, doi: 10.1109/JPROC.2012.2190168.
- [2] K. Cherenack and L. Van Pieterse, "Smart textiles: Challenges and opportunities," *Journal of Applied Physics*, vol. 112, no. 9, p. 091301, May 2012, doi: 10.1063/1.4742728.
- [3] S. Lee, S. Jeon, R. Chaji, and A. Nathan, "Transparent Semiconducting Oxide Technology for Touch Free Interactive Flexible Displays," *Proceedings of the IEEE*, vol. 103, no. 644, pp. 644–664, May 2015, doi: 10.1109/JPROC.2015.2405767.
- [4] S. Bauer, "Flexible electronics: Sophisticated skin," *Nature Materials*, vol. 12, no. 10, pp. 871–872, September 2013, doi: 10.1038/nmat3759.
- [5] G. Park, H. J. Chung, K. Kim, S. A. Lim, J. Kim, Y. S. Kim, Y. Liu, W. H. Yeo, R. H. Kim, S. S. Kim, J. S. Kim, Y. H. Jung, T. il Kim, C. Yee, J. A. Rogers, and K. M. Lee, "Immunologic and tissue biocompatibility of flexible/stretchable electronics and optoelectronics," *Advanced Healthcare Materials*, vol. 3, no. 4, pp. 515–525, April 2014, doi: 10.1002/adhm.201300220.
- [6] K. Nomura, H. Ohta, A. Takagi, T. Kamiya, M. Hirano, and H. Hosono, "Room-temperature fabrication of transparent flexible thin film transistors using amorphous oxide semiconductors," *Nature*, vol. 432, no. 7016, pp. 488–492, November 2004, doi: 10.1038/nature03090.
- [7] G. Cantarella, C. Vogt, R. Hopf, N. Münzenrieder, P. Andrianakis, L. Petti, A. Daus, S. Knobelspies, L. Büthe, G. Tröster, G. A. Salvatore, "Buckled Thin-Film Transistors and circuits on soft elastomers for stretchable electronics," *ACS applied materials & interfaces*, vol. 9, no. 34, pp. 28750–28757, August 2017, doi: 10.1021/acsami.7b08153.
- [8] L. Petti, N. Münzenrieder, C. Vogt, H. Faber, L. Büthe, G. Cantarella, F. Bottacchi, T. D. Anthopoulos, and G. Tröster, "Metal oxide semiconductor thin-film transistors for flexible electronics," *Applied Physics Reviews*, vol. 3, no. 2, p. 021303, June 2016, doi: 10.1063/1.4953034.
- [9] N. Münzenrieder, L. Petti, C. Zysset, T. Kinkeldei, G. A. Salvatore, and G. Tröster, "Flexible self-aligned amorphous InGaZnO thin-film transistors with sub-micrometer channel length and a transit frequency of 135 MHz," *IEEE Transaction on Electron Devices*, vol. 60, no. 9, pp. 2815–2820, August 2013, doi: 10.1109/TED.2013.2274575.
- [10] L. Petti, P. Aguirre, N. Münzenrieder, G. A. Salvatore, C. Zysset, A. Frutiger, L. Büthe, C. Vogt, and G. Tröster, "Mechanically flexible vertically integrated a-IGZO Thin-Film Transistors with 500 nm channel length fabricated on free standing plastic foil," *IEEE International Electron Devices Meeting (IEDM)*, pp. 11.4.1–11.4.4, December 2013, doi: 10.1109/IEDM.2013.6724609.
- [11] L. Petti, A. Frutiger, N. Münzenrieder, G. A. Salvatore, L. Büthe, C. Vogt, G. Cantarella, G. Tröster, "Flexible quasi-vertical In-Ga-Zn-O thin-film transistor with 300-nm channel length," *IEEE Electron Device Letters*, vol. 36, no. 5, pp. 475–477, March 2015, doi: 10.1109/LED.2015.2418295.
- [12] N. Münzenrieder, G. A. Salvatore, L. Petti, C. Zysset, L. Büthe, C. Vogt, G. Cantarella, and G. Tröster, "Contact resistance and overlapping capacitance in flexible sub-micron long oxide thin-film transistors for above 100 mhz operation," *Applied Physics Letters*, vol. 105, no. 26, p. 263504, December 2014, doi: 10.1063/1.4905015.
- [13] M. Thiel, J. Fischer, G. von Freymann, and M. Wegener, "Direct laser writing of three-dimensional submicron structures using a continuous-wave laser at 532 nm," *Applied Physics Letter*, vol. 97, no. 22, pp. 221102 1–3, November 2010, doi: 10.1063/1.3521464.
- [14] N. Lindenmann, G. Balthasar, D. Hillerkuss, R. Schmögrow, M. Jordan, J. Leuthold, W. Freude, and C. Koos, "Photonic wire bonding: a novel concept for chip-scale interconnects," *Optics Express*, vol. 20, no. 16, pp. 17667–17677, July 2012, doi: 10.1364/OE.20.017667.
- [15] J. K. Gansel, M. Latzel, A. Frölich, J. Kaschke, M. Thiel, and M. Wegener, "Tapered gold-helix metamaterials as improved circular polarizers," *Applied Physics Letter*, vol. 100, no. 10, p. 101109, February 2012, doi: 10.1063/1.3693181.
- [16] M. A. Zeeshan, R. Grisch, E. Pellicer, K. M. Sivaraman, K. E. Peyer, J. Sort, B. Özkale, M. S. Sakar, B. J. Nelson, and S. Pané, "Hybrid helical magnetic microrobots obtained by 3d template assisted electrodeposition," *Small*, vol. 10, no. 7, pp. 1284–1288, December 2014, doi: 10.1002/smll.201302856.
- [17] M. Röhrig, M. Thiel, M. Worgull, and H. Hölscher, "Hierarchical structures: 3d direct laser writing of nano- and microstructured hierarchical gecko-mimicking surfaces," *Small*, vol. 8, no. 19, pp. 2918–2918, July 2012, doi: 10.1002/smll.201200308.
- [18] E. Blasco, J. Müller, P. Müller, V. Trouillet, M. Schön, T. Scherer, C. Barner-Kowollik, and M. Wegener, "Fabrication of conductive 3d gold-containing microstructures via direct laser writing," *Advanced Materials*, vol. 28, no. 18, pp. 3592–3595, March 2016, doi: 10.1002/adma.201506126.
- [19] L. Petti, "Metal oxide semiconductor thin-film transistors for flexible electronics", *Ph.D. dissertation*, Dept. Elect. Eng. And Inf. Tech., ETH Zurich, Zurich, 2016, doi: 10.3929/ethz-a-010668974.
- [20] S. Hengsbach and A. D. Lantada, "Direct laser writing of auxetic structures: present capabilities and challenges," *Smart Materials and*

*Structures*, vol. 23, no. 8, p. 085033 1-10, July 2014, doi: 10.1088/0964-1726/23/8/085033.

- [21] F. Klein, T. Striebel, J. Fischer, Z. Jiang, C. M. Franz, G. Von Freymann, M. Wegener, and M. Bastmeyer, "Elastic fully three dimensional microstructure scaffolds for cell force measurements," *Advanced Materials*, vol. 22, no. 8, pp. 868–871, January 2010, doi: 10.1002/adma.200902515.
- [22] A. Ostendorf and B. N. Chichkov, "Two-photon polymerization: a new approach to micromachining," *Photonics Spectra*, vol. 40, no. 10, p. 72, October 2006.
- [23] L. Petti, N. Münzenrieder, G. A. Salvatore, C. Zysset, T. Kinkeldei, L. Büthe, G. Tröster, "Influence of mechanical bending on flexible InGaZnO-based ferroelectric memory TFTs," *IEEE Transaction on Electron Devices*, vol. 61, no. 4, pp. 1085–1092, March 2014, doi: 10.1109/TED.2014.2304307.
- [24] D. A. Neamen, "Electronic Circuit Analysis and Design", 1996.
- [25] D. Lovelace, J. Costa, and N. Camilleri, "Extracting small-signal model parameters of silicon MOSFET transistors," in *IEEE International Microwave Symposium Digest (MTT-S)*, vol. 2, pp. 865–868, May 1994, doi: 10.1109/MWSYM.1994.335220.
- [26] H. Gleskova, S. Wagner, and Z. Suo, "a-Si:H thin film transistors after very high strain," *Journal of Non-Crystalline Solids*, vol. 266–269, pp. 1320–1324, May 2000, doi: 10.1016/S0022-3093(99)00944-8.



**Luisa Petti** (S'12-M'16) received the M.Sc. degree in electronic engineering from Politecnico di Milano in 2011, and the Ph.D. degree in electrical engineering and information technology from ETH Zurich in 2016.

Her current research interests include the

fabrication and characterization of flexible metal oxide thin-film devices and circuits.



**Emanuel Greco** received the M.Sc degree in electronic engineering from Swiss Federal Institute of Technology (ETH) Zurich in 2015. He is currently employed as hardware developer for TEM AG, Chur, Switzerland.



**Giuseppe Cantarella** received the M.Sc degree in electronic engineering from Polytechnic of Turin, Turin, Italy, Grenoble INP, Grenoble, France and École Polytechnique Fédérale de Lausanne, Lausanne, Switzerland in 2013. Since 2013, he has been pursuing

the Ph.D. degree with ETH Zurich, Switzerland. His current research interests include flexible and stretchable electronics.



**Niko Münzenrieder** (S'11-M'14) received the Diploma degree in physics from the Technical University Munich, Munich, Germany, in 2008, and the Ph.D. in electrical engineering from ETH Zurich, Zurich, Switzerland, in 2013.

He is currently a Lecturer with the University of Sussex, Brighton, U.K., where he is involved in flexible and

stretchable thin-film electronics.



**Christian Vogt** (S'14) received the M.Sc. degree in electrical engineering and information technology from the Swiss Federal Institute of Technology (ETH) Zurich in 2013, where he obtained his Ph.D degree in 2017.

His current research interests include flexible electronics and applications for magnetic resonance imaging.



**Gerhard Tröster** (SM'93) has been a Full Professor of Electronics with the ETH Zurich, Zurich, since 1993. His current research interest include signal processing, wireless sensor networks, wearable computing, smart textiles applying flexible, and organic electronics.